






RESEARCH ARTICLE | MAY 08 2024

Asymmetric aerosol volume transmission: A computational approach toward infection prevention efficiency of face masks

Special Collection: [Flow and the Virus](#), [Flow and the Virus](#)

D. A. Matthijs de Winter ; Frank M. Verhoeven ; Lucie C. Vermeulen ; Erwin Duizer ; Alvin A. Bartels; Ana Maria de Roda Husman; Jack F. Schijven 



Physics of Fluids 36, 051902 (2024)

<https://doi.org/10.1063/5.0204150>



APL Energy
Latest Articles Online!
Read Now

Asymmetric aerosol volume transmission: A computational approach toward infection prevention efficiency of face masks

Cite as: Phys. Fluids **36**, 051902 (2024); doi: [10.1063/5.0204150](https://doi.org/10.1063/5.0204150)

Submitted: 20 February 2024 · Accepted: 22 April 2024 ·

Published Online: 8 May 2024



View Online



Export Citation



CrossMark

D. A. Matthijs de Winter,^{1,a)}  Frank M. Verhoeven,^{2,b)}  Lucie C. Vermeulen,¹  Erwin Duizer,¹  Alvin A. Bartels,¹
Ana Maria de Roda Husman,^{1,3} and Jack F. Schijven^{1,4} 

AFFILIATIONS

¹Centre for Infectious Disease Control, National Institute for Public Health and the Environment, Bilthoven 3721 MA, The Netherlands

²Medspray B.V., 7521 PV, Enschede, The Netherlands.

³Institute for Risk Assessment Sciences, Utrecht University, 3584 CL Utrecht, The Netherlands

⁴Environmental Hydrogeology, Department of Earth Sciences, Utrecht University, 3584 CS Utrecht, The Netherlands

Note: This paper is part of the special topic, Flow and the Virus.

^{a)}Author to whom correspondence should be addressed: matthijs.de.winter@rivm.nl

^{b)}Present address: Resyca B.V., 7521 PV, Enschede, The Netherlands.

ABSTRACT

Wearing face masks is considered as one of the infection prevention and control options for respiratory viruses (e.g., SARS-CoV-2) that acts by blocking virus-laden aerosols. It is generally thought that aerosol blockage occurs when air passes through the face mask fabric. We calculated air flows through face masks and through peripheral leakages, based on reported breathing resistance values of face masks (FFP/N95, surgical masks, and cloth masks) and found that most of the inhaled and exhaled air passes through these peripheral leakages. Nevertheless, face masks remain effective as an infection prevention option, because additional calculations showed that the majority of aerosol volume cannot follow the tortuous path of air around the face mask. The filtering efficiency through the peripheral leakages can be described as a function of breathing conditions, vocal activities, the leakage geometry and tortuous pathway, aerosol properties (diameter, composition) and ambient conditions (e.g., evaporation, ventilation). Inclusion of these parameters explains the asymmetric filtering behavior of face masks, i.e., the risk of infection from person A to person B does not necessarily equal the risk of infection from person B to person A. Our findings explain thus why masking an infectious person is more effective than masking an exposed person. Establishing that the tortuous pathway of air around the face mask is the sole contributor to face mask efficiency opens new opportunities for designing safer face masks.

© 2024 Author(s). All article content, except where otherwise noted, is licensed under a Creative Commons Attribution (CC BY) license (<https://creativecommons.org/licenses/by/4.0/>). <https://doi.org/10.1063/5.0204150>

I. INTRODUCTION

The SARS-CoV-2 pandemic starting at the end of 2019 led to an unprecedented increase in face mask use by the general public on a global scale, resulting in a major environmental burden.^{1,2} Notwithstanding, face masks are considered as one of the most important infection prevention tools against the spreading of SARS-CoV-2,^{3,4} a necessity in particular, before the vaccines became available, and still important with the emergence of new variants of concern and the general prospects of outbreaks of new respiratory pathogens with the potential of pandemic proportions.

Global shortages of FFP masks (i.e., similar to N95 and KN95) and surgical masks (SMs) led to a surge in scientific work related to

testing cloth community face masks,^{5–8} and FFP masks/SM,^{5,8–12} including reuse^{13,14} of face masks for their efficiency in preventing the inhalation and exhalation of virus-laden aerosols. We note that the intended use for SM (primarily source control, loose fit, mainly blocking large droplets) is different from the intended use of FFP masks (protecting the wearer, sealing around the edges, blocking aerosols). It is crucial to understand the face mask design parameters and choice of materials in relation to the protection efficiency and to enable the development of face masks with a smaller environmental footprint.

Epidemiological studies have found a reduced risk of SARS-CoV-2 infections when comparing wearing a face mask vs no mask in community settings, although the strength of evidence is considered low to

moderate due to methodological limitations, such as recall bias.¹⁵ For example, the CDC published adjusted odd ratios of 0.51 [95% confidence interval (CI) = 0.29–0.93] for the probability of receiving a positive for SARS-CoV-2 test after wearing a face mask indoors versus not wearing a face mask indoors, and further specified for surgical masks (SMs) 0.34 (95% CI = 0.13–0.90), N95/K95 respirators 0.17 (95% CI = 0.05–0.64), and cloth masks (although statistically not significant) 0.44 (95% CI = 0.17–1.17)¹⁶. Deterministic epidemiology modeling studies have indicated that a moderate functionality (i.e., blocking viruses moderately effective) of face masks would already have a significant effect on virus spreading across a community,¹⁷ seemingly in contradiction with the wide confidence intervals reported in epidemiological studies. A confidence interval upper limit close to unity implies that it is possible that face masks do not have a protective effect. When translating the epidemiological data to the level of individuals, it appears that the face mask protection efficiency for indoor situations varies strongly, which points toward the complexity of the virus transmission process and insufficiently constrained.

Variations in infection prevention effectivity at a personal level contradict standardized laboratory tests of FFP face mask fabrics, generally scoring very high (90%–99%) on aerosol filter efficiencies^{18–20} when challenged with aerosols containing salt crystallites. However, measurements of expelled virus concentrations through face masks, either worn by volunteers or placed on opposing mannequins, result in up to tens of percentages lower efficiencies.^{21–24} The limitation of the face mask capability in blocking virus-laden aerosols in practice is attributed to peripheral leakages, i.e., leakages around the face seal.^{25–29} A common suggestion is that a proper fit would overcome the leakages and improve infection prevention effectiveness. However, it was recently noticed that the high breathing resistance of face masks would actually require leakages to allow breathing.³⁰ Work by Chuanxin and co-workers²⁹ showed that peripheral leakages do not directly imply a poor functioning face mask. Although the air flows around the face mask, the aerosols potentially containing the virus are unable to follow the air flow.

Building on the significance of peripheral leakage, here we present a reduced-order model to calculate the effectivity of aerosol blockage despite the peripheral leakages. By realizing that air carrying the aerosols must navigate along a tortuous pathway around the edges of the face masks, it is the inertia of the aerosols (i.e., Stokes number²⁹) that drives them against the face mask or skin. The extent of aerosols hitting the face mask or skin depends mainly on the air flow velocity and the mass of aerosols.

The air flow varies continuously during each breathing cycle. Therefore, the first part of our model computes the air flow velocities during one minute of breathing (both inhalation and exhalation). The second part of the model computes the corresponding filter efficiencies, providing a new and unique insight into the actual filter mechanism of face masks and relates the filter efficiency to breathing dynamics and aerosol size and composition characteristics. Moreover, the models allow studying specific situations (i.e., room conditions, people’s activities, masking the source and/or masking the exposed) and explain why face masks have a variable infection prevention efficiency, depending on the circumstances. Our findings have direct consequences for future developments of face masks with an improved infection prevention effectiveness and a smaller environmental footprint and improved sustainable prospects.

II. METHODS

First, the description of the lung model is provided, which has been used to simulate air flows in and out of the mouth. A crucial part of the lung model is the permeability of the face mask and the permeability of the peripheral leakages. Second, the aerosol capture model is described, which calculates the change in aerosol size distribution by wearing a face mask. Part of the aerosol capture model describes exhaled aerosol size distributions.

A final step involves combining both models and calculating aerosol volume transmission between an infectious person and an exposed person. The aerosol volume transmission constitutes the transmitted volume (in picolitres) of aerosols per minute. The number of virus particles in an aerosol is considered proportional to the volume of the aerosol, assuming that the concentration of virus particles in aerosols remains the same for small and large aerosols. However, the concentration of aerosols varies over many orders of magnitude (10^2 – 10^8 virus/ml),³¹ due to different stages of the infection and different levels of severity of the infection. Therefore, this study focuses on the effect of face masks on the transmission of aerosol volumes and not on the number of virus particles.

A. Modified lung model

1. Modified lung model description

To capture the breathing dynamics, a mathematical model of the lung was used.³² Air flowing in and out of a pair of lungs constitutes a pneumatic system, which can be modeled with an electrical circuit analogy.³³ The pressure applied by respiratory muscles to the diaphragm (p_{muscle}) is analogous to voltage. The air ways resistances ($\text{Pa s}^{-1} \text{m}^{-3}$) are analogous to electrical resistances and the compliances ($\text{m}^3 \text{Pa}^{-1}$) are analogous to capacitances. Accordingly, a lung model was adopted,³² which is depicted in Fig. 1. The modification consisted of two additional, parallel resistors. One resistor represented the face mask fabric, and the second resistor represented the peripheral leakages.

The input signal p_{muscle} was defined as³²

$$p_{\text{muscle}}(t) = \begin{cases} \frac{-p_{\text{mus,min}} t^2 + \frac{p_{\text{mus,min}} T_{\text{cycle}}}{T_I T_E} t}{T_I T_E} & \text{inhalation: } t \in [0, T_I], \\ \frac{p_{\text{mus,min}}}{1 - e^{-\frac{T_I}{\tau}}} \left(e^{-\frac{t-T_I}{\tau}} - e^{-\frac{T_I}{\tau}} \right) & \text{exhalation: } t \in [T_I, T_{\text{cycle}}]. \end{cases} \quad (1)$$

As indicated, two complementary functions were used to calculate the inhalation phase T_I and the exhalation phase T_E , respectively, as a function of time t (all in seconds). The sum of T_I and T_E is the total time T_{cycle} , in seconds, of a single respiratory cycle. The exponential respiratory profile is determined by the time constant τ .

In the literature, a common value to report is the respiration rate RR (breaths/min), which is related to T_I , T_E , and T_{cycle} according to

$$T_I + T_E = T_{\text{cycle}} = \frac{60}{RR}. \quad (2)$$

A second common value reported in the literature is the inhalation–exhalation time ratio IE_{ratio} :

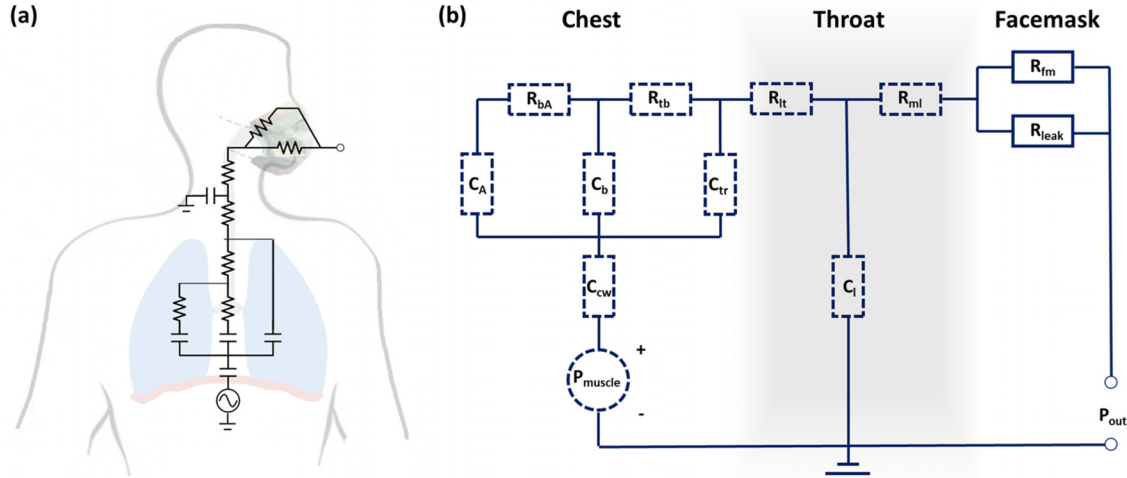


FIG. 1. The adopted lung model³² (a) as a conceptual model and (b) with the specific components explained: The dashed components depict the original model, with the same notation: P_{muscle} is the input pressure, C_{CW} is the compliance of the chest wall, C_A is the compliance of alveoli, C_b is the compliance of the bronchia, C_{tr} is the compliance of the trachea, R_{bA} is the air flow resistance between the bronchia and alveoli, R_{tb} is the air flow resistance between the trachea and bronchia, R_{lt} is the air flow resistance between larynx and the trachea, C_l is the compliance of the larynx, and R_{ml} is the air flow resistance between the mouth opening and the larynx. The additional facemask consists of two parallel resistances. R_{fm} is the air flow resistance through the face mask and R_{leak} is the air flow resistance of the leakage (air flow around the facemask). For the parameter values, see Table I.

TABLE I. Parameter values for the lung model for tidal breathing.³²

Compliance ($\text{m}^3 \text{Pa}^{-1}$)	Air flow resistance ($\text{Pa s}^{-1} \text{m}^{-3}$)	Additional parameters
$C_l = 1.30 \times 10^{-8}$	$R_{ml} = 1.00 \times 10^5$	RR = 12 breaths/min
$C_t = 2.43 \times 10^{-8}$	$R_{lt} = 3.30 \times 10^4$	$IE_{\text{ratio}} = 0.6$
$C_b = 1.34 \times 10^{-7}$	$R_{tb} = 3.00 \times 10^4$	$\tau = T_E/5$
$C_A = 2.04 \times 10^{-6}$	$R_{bA} = 8.01 \times 10^4$	
$C_{\text{CW}} = 2.49 \times 10^{-6}$		

$$\frac{T_I}{T_E} = IE_{\text{ratio}}. \tag{3}$$

The numerical values of the parameters are provided in Table I.

The pressure within the oral cavity was assumed to be equal to the pressure between the face and face mask. This assumption would be potentially incorrect during nasal breathing and blowing/whistling. In the latter case, lips are almost sealing the oral cavity, creating a pressure difference between the oral cavity and the ambient room. For tidal

breathing or breathing during physical exercises, it was assumed that the mouth is sufficiently opened to ensure equal pressure between the oral cavity and the face mask.

With P_{out} kept at zero (i.e., the pressure in the room does not change due to breathing of an individual), air flows through and around the mask can be calculated as a function of time.

2. Evaluating the modified lung model

The evaluation of the electric circuit-analogue of the respiratory system (Fig. 1) was done by Modified Nodal Analysis (MNA).³⁴ Each connection between two or more network components (e.g., R_{bA} , R_{tb} , and C_b) is called a node. According to Kirchhoff's current law (KCL), the sum of electrical currents flowing in and out of a node must be zero (assuming steady state), which is analogous to the conservation of mass in the case of air flow. The electrical current i through a component is provided by Ohm's law: $i(t) = u(t)/R$, where u is the voltage across resistor R . Instead of R , the impedance Z is used ($Z_R = R$; $Z_C = 1/s$) through a Laplace transformation, where s is the complex frequency. Applying KCL to all the nodes in the network results in a system of linear equations. Collecting the coefficients results in

$$[G + sC] = \begin{bmatrix} sC_{cw} & -sC_{cw} & 0 & 0 & 0 & 0 & 0 & 0 & -1 \\ -sC_{cw} & s(C_A + C_B + C_{cw} + C_{tr}) & -sC_A & -sC_B & -sC_{tr} & 0 & 0 & 0 & 0 \\ 0 & -sC_A & G_{bA} + sC_A & -G_{bA} & 0 & 0 & 0 & 0 & 0 \\ 0 & -sC_B & -G_{bA} & G_{bA} + G_{tb} + sC_B & -G_{tb} & 0 & 0 & 0 & 0 \\ 0 & -sC_{tr} & 0 & -G_{tb} & G_{lt} + G_{tb} + sC_{tr} & -G_{lt} & 0 & 0 & 0 \\ 0 & 0 & 0 & 0 & -G_{lt} & G_{lt} + G_{ml} + sC_L & -G_{ml} & 0 & 0 \\ 0 & 0 & 0 & 0 & 0 & -G_{ml} & G_{ml} + G_{fm} + G_{leak} & 0 & 0 \\ 1 & 0 & 0 & 0 & 0 & 0 & 0 & 0 & 0 \end{bmatrix}, \tag{4}$$

where the “1” and “−1” elements represent the input current. Collecting the voltages at each node and the input current into a vector $\mathbf{X}(s)$ allows us to write

$$[\mathbf{G} + s\mathbf{C}]\mathbf{X}(s) = \mathbf{B}\mathbf{I}_{input}(s). \quad (5)$$

Similarly, the output vector $\mathbf{Y}(s)$ is described as follows:

$$\mathbf{Y}(s) = \mathbf{T}\mathbf{X}(s), \quad (6)$$

where the vector $\mathbf{I}_{input}(s)$ represents the input signals with coefficients listed in vector \mathbf{B} . Likewise, the output vector $\mathbf{Y}(s)$ equals the vector $\mathbf{X}(s)$ with voltages and currents multiplied with the vector \mathbf{T} assigning the output node.

Of interest is the transfer function $H(s)$, which relates the output signal to any arbitrary input signal [$H(s) = Y(s)/X(s)$]. By combining Eqs. (5) and (6), we obtain

$$H(s) = \frac{Y(s)}{X(s)} = \mathbf{T}[\mathbf{G} + s\mathbf{C}]^{-1}. \quad (7)$$

Inverting the matrix in Eq. (4) was done symbolically in MATLAB (version R2018a), resulting in a quotient with polynomials in the nominator and denominator. The actual result is too bulky to be suitable for print.

Following the derivation of $H(s)$ for the modified lung model, any output pressure can be computed, based on an arbitrary input pressure through $H(s)$. In MATLAB, we used the “lsim” function to compute the resulting output pressures $p_{out}(t)$, which takes the transfer function $H(s)$, the input signal $p_{muscle}(t)$, and a vector with time (we used a 10-ms time interval).

By computing the output pressure in the oral cavity and assuming the ambient pressure to be constant, a time-dependent pressure difference across the face mask was determined, from which the flow was calculated (see Sec. II A 3).

3. Air flow resistances

Fluid (e.g., air) transportation through a porous material such as a face mask can be described by Darcy’s law:

$$Q = \frac{kA}{\mu L} \Delta p, \quad (8)$$

where A is the surface area (m^2), L is the thickness (m), μ is the dynamic viscosity of air (Pa s), k is the permeability of the face mask (m^2), Δp is the pressure difference or pressure drop across the face mask (Pa), and Q is the flow through the face mask ($m^3 s^{-1}$). The temperature- and pressure-dependent dynamic viscosity of air is provided in the supplementary material.

Darcy’s law strongly resembles Ohm’s law. Therefore, an air flow resistance value R ($Pa s^{-1} m^{-3}$) suitable for the lung model is defined as follows:

$$R = \frac{\mu L}{kA}. \quad (9)$$

The air flow resistance of the face mask is a function of its dimensions (A , L), properties of air (μ), and the properties of the face mask (k). The air flow velocity as a function of time $u(t)$ through the mask and through the peripheral leakages can be calculated from the pressure drop, based on Darcy’s law [Eq. (8)], where $u(t) = Q(t)/A$.

4. Minute ventilation

An additional lung model output parameter was reviewed for comparison with the literature: The total volume of inhaled air during one minute of breathing (known as minute ventilation V_E , in $m^3 \text{min}^{-1}$ or $l \text{min}^{-1}$). The volume of air moving through a cross-sectional area A with variable velocity $u(t)$ was calculated by integrating the velocity over time. The cross-sectional area A (m^2) is the total surface area of the peripheral leakage (Sec. II A 3). In this work, the velocity profile was a discrete function $u[n]$ with a time interval Δt (0.01 s),

$$V_E = A \sum_1^{60/\Delta t} u[n] \Delta t \quad \text{for all } u[n] < 0. \quad (10)$$

The restriction of $u[n] < 0$ excludes exhalation (which is $u[n] > 0$), as minute ventilation is the sum of inhaled air. Integrating a full breathing cycle would result in zero volume as the inhaled minute ventilation equals the exhaled minute ventilation.

The time-dependent air flow velocity profile $u(t)$ through the face mask and through the peripheral leakages has been established as a function of the air flow resistance. Next is a description of the model for the aerosols following the air flow.

B. Aerosol capture model

The aerosol capture efficiency was defined as the fraction of aerosols that are captured by a filter, in this case either by the face mask itself or within the peripheral leakages around the face mask. The presented aerosol capture model is based on the work by Borgelink *et al.*, 2022.³⁵ The main difference from the present study is that the filtering by electrostatic capture was ignored in this study because the present study considered air flow primarily through the peripheral leakages for which the role of electrostatic capture has not been characterized (follows from Sec. III). Electrostatic captures appear effective mainly for the smaller ($< 1 \mu m$) aerosols,³⁵ which would justify a pragmatic approach of not-including electrostatic interactions, as explained in Sec. III on aerosol size distribution profiles.

The aerosol capture model has been developed for fibrous porous materials such as face masks. The model starts with estimating the probability of a particle or aerosol to collide with a single fiber. Any collision with a fiber implies a “capture,” i.e., the aerosol becomes permanently attached to the fiber.

Woven or non-woven filters generally consist of a large number of single fibers. The work of Borgelink *et al.*³⁵ includes a final summation over the stack of fibers. In order to calculate the effect of peripheral leakages and potential air flow through the peripheral leakages and thus around the face mask edges, we considered the edge of the face mask as a (large) “single fiber.”

The full mathematical description of the aerosol capture model can be found in the supplementary material.

C. Aerosol diameter distributions

The aerosol size distribution for breathing was extracted from Fig. 5 from Fabian.³⁶ Similarly, data for breathing, speaking, and singing were extracted from Fig. 2 from Alsved.³⁷ Power laws were fitted to the data, resulting in diameter-dependent aerosol concentration (#particles/l) curves for exhaled air. The bin size of the aerosol diameters in the present work is 50 nm (range: 0.1–1 μm) and 100 nm (range: 1–20 μm),

which is much smaller than the bin sizes in the work of Fabian. A bin-size correction is applied by normalizing the sum over the aerosols over all diameters from this study to the sum over all aerosols from Fabian.³⁶ The original data from Alsvéd³⁷ provided exhaled aerosols per second. The power law fitted to the original breathing curve was normalized to the breathing curve from Fabian³⁶ (based on total numbers of aerosols). The normalization factor applied to the breathing curve from Alsvéd was also applied to the curve fits of the speaking and singing data.

It is assumed that the number of virus particles in aerosols correlates linearly with the aerosol volume. Therefore, the #particle/l distributions are recalculated into picoliter (pl) aerosol/l distributions. When calculating the volume of aerosols, it was assumed that aerosols are spherical. The volume of aerosols per liter of air follows from the volume of a single aerosol with a particular diameter, multiplied by the abundance of that aerosol.

D. Coupling lung and aerosol capture model

The lung model produced a 60 s (time step of 10 ms) air velocity profile through the face mask and through the peripheral leakages. The velocity profile was used as input for the aerosol capture model. The combination resulted in a fraction of captured aerosols as a function of aerosol diameter, per time step, which functions as further input for characterizing the face mask efficiency and for the aerosol volume transmission model.

E. Aerosol volume transmission model

A conceptual model of aerosol volume transmission from an infectious person to an exposed person is depicted in Fig. 2. The coupled lung and aerosol capture models were applied to both an infectious person, considering exhalation only, and an exposed person, considering inhalation only. Quantification of the schematic plots follows from the model results and is shown in Sec. III (Fig. 8).

In Fig. 2, the inhaled volume of aerosols by the exposed person (VI) is the product of six preceding modifications of the original exhaled diameter-dependent aerosol distribution (I), depicted in the schematic log-log plots. The combination of the breathing dynamics and the face mask leakages on both the infectious (II) and exposed (V) person lowers the concentrations of aerosols, where the reduction factor is a function of the aerosol diameter.

An additional factor is the impact of ambient conditions (e.g., room ventilation), as it has a strong influence on the aerosol size distribution:

1. Ambient temperature and relative humidity: Exhaled aerosols undergo partial evaporation once they have passed the face mask, resulting in a reduction η of 0.8–0.2 of their original diameters, depending on the relative humidity^{48,49} [Fig. 2(III)]. Consequently, the viral concentration in partially evaporated aerosols increases by a factor $1/\eta^3$. Smaller aerosols are more likely to pass around the face mask, which is at this point of relevance to the exposed, inhaling person. Evaporation provides an additional explanation for the asymmetric protection efficiency

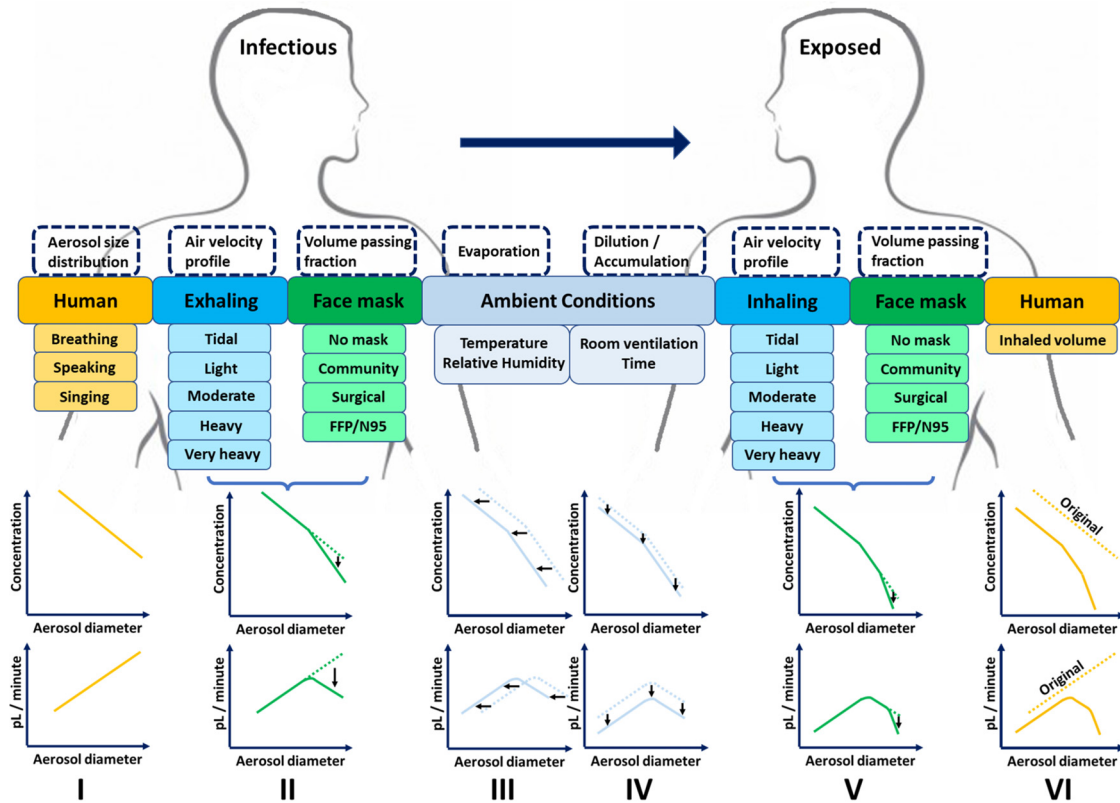


FIG. 2. The conceptual model for the exchange of aerosols, with log-log plots based on concentration and aerosol volume.

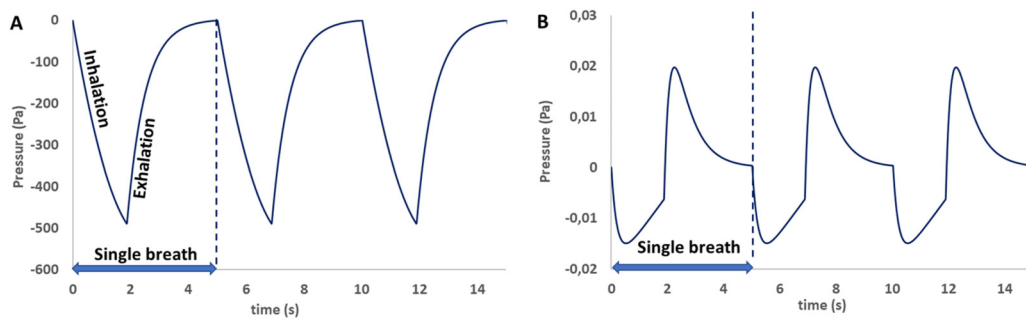


FIG. 3. Breathing cycles from the pressure input signal (a) through the electrical network analogue of the respiratory system to the oral cavity pressure (b). The pressure difference between the oral cavity and the surroundings is small due to the effective peripheral leakages.

- between exhalation and inhalation, with masking a source (infectious person) being more effective than masking an exposed person.^{21–24} Our work did not include the virus load in aerosols. Instead of increasing the virus concentration, we multiplied the inhaled aerosol volume by $1/\eta^3$ to a hypothetical “equivalent volume” with the same absolute number of virus particles. All calculations were performed with $\eta = 0.35$.
2. Room ventilation and time: We appreciate that proximity, room ventilation rates, and air circulation have a strong additional impact on the temporal evolution of the aerosol concentration in front of an exposed person. Ventilation and dilution by the volume of the room lowers the concentration [Fig. 2(IV)], albeit that the opposite effect is achieved by accumulation in a non-ventilated room. Gravitational settling of aerosols in time scales with the aerosol radius square, resulting in the largest aerosols settling the fastest. Ventilation and temporal effects of the room on the distribution are beyond the scope of our research.

III. RESULTS

A. Permeability face masks

Experimental publications often report pressure drops and corresponding air flows, instead of permeability values. It is not always possible to calculate the permeability of the face mask due to missing face mask properties (thickness, surface area of the measurement).

Table II lists a number of permeability values calculated from the literature by using Darcy’s law [Eq. (8)]. Literature-based permeability values for surgical masks vary from $\sim 2.0 \times 10^{-11}$ to $\sim 3.4 \times 10^{-13} \text{ m}^2$ (median value = $1.1 \times 10^{-11} \text{ m}^2$) for SM, and from $\sim 1.4 \times 10^{-11}$ to $\sim 2.5 \times 10^{-13} \text{ m}^2$ (median value = $2.7 \times 10^{-12} \text{ m}^2$) for FFP/N95 face masks. It is noticed that the permeability of the surgical mask is less than that of the FFP mask, but the pressure drop is typically smaller for the surgical mask in comparison to the FFP mask, which is a direct consequence of the difference in thickness between the two masks. Therefore, the air flow resistance remains similar. The overall permeability values are surprisingly small.

In Sec. III B, the permeability values are applied in the modified lung model.

B. Breathing with a face mask

1. Minute ventilation without peripheral leakages

The evaluation of the modified lung model is shown in Fig. 3 for tidal breathing conditions. The pressure created by the diaphragm is

shown in Fig. 3(a) and the resulting pressure difference across the face mask is shown in Fig. 3(b), as discussed in Sec. III B 2.

Table III shows the minute ventilation (l min^{-1}) [Eq. (10)] for several pressures from the respiratory muscles (kPa) and respiratory rates (breaths min^{-1}) calculated by our model. The increase in both pressure and RR occurs during physical exercises.³⁸

We calculated the minute ventilation through face masks without leakages and covering the full range of permeability values (Table II) and compared the volume of inhaled air with the volume of air that would be inhaled without a face mask. We found a reduction in minute ventilation of $<1\%$ (tidal breathing conditions for $V_E = 6.5 \text{ l min}^{-1}$, $k_{fm} = 2.0 \times 10^{-11} \text{ m}^2$) up to 78% (moderate work conditions for $V_E = 35 \text{ l min}^{-1}$, $k_{fm} = 2.5 \times 10^{-13} \text{ m}^2$). Given the wide range of permeability values, we also calculated the minute ventilation reduction for average input values (light work conditions for $V_E = 20 \text{ l min}^{-1}$, $k_{fm} = 2.7 \times 10^{-12} \text{ m}^2$) to be 11%. In the latter case, inhaling 11% less volume air per minute translates directly to 11% less oxygen available for uptake by the lungs and also less CO_2 carried away during exhalation, per minute, which will be experienced as shortness of breath.

Wearing a face mask should not affect, or should affect as little as possible, the physical effort to breathe (e.g., oxygen levels and heart and breathing rate),³⁹ which led us to postulate the following modeling condition: *Breathing parameters and the resulting minute ventilation should remain unchanged when wearing a face mask with peripheral leakages.*

Section III B 2 adds peripheral leakages and examines the possibility to make up for the reduction in minute ventilation.

2. Minute ventilation with peripheral leakages

Adding peripheral leakages requires knowledge of the geometry of peripheral leakages. A CT-study (computed tomography, spatial resolution of $75 \mu\text{m}$) revealed that the peripheral leakages consist of small openings along the face mask perimeter.⁴⁰ The total surface area of the peripheral leakage was found to range from 0.2% to 2.6% of the entire surface area of the face mask (with a mean of 0.8%). The variation was caused by measuring three different types of N95 face masks and putting the face masks on three differently sized manikins. To place these values in perspective, 0.8% of 0.0163 m^2 (total surface area of a face mask) is approximately 1.3 cm^2 . Assuming a face mask with a circumference of 24 cm results in an average distance of 0.5 mm between the face mask and the facial skin. A peripheral leakage surface

TABLE II. Permeability values derived from various literature sources for surgical masks and FFP/N95/KN95 masks.

SM = surgical mask, DPM = disposable mask		
Study	Mask description	Permeability (m ²)
Du ¹	SM	3.40×10^{-13}
Duncan ²	DPM (Henan Liwei)	8.77×10^{-12}
	DPM (PG4-1200)	1.12×10^{-11}
	DPM (PG4-1273)	1.79×10^{-11}
	DPM (Vanche)	1.03×10^{-11}
	DPM (PG4-2001)	1.64×10^{-11}
	DPM (PG4-2331)	2.03×10^{-11}
Varanges ³	SM/reference	1.11×10^{-11}
	SM/folded	1.14×10^{-11}
	SM/sweat	1.10×10^{-11}
	SM/saliva	1.14×10^{-11}
	SM/washed	1.21×10^{-11}
Ayodeji ⁴	SM	1.98×10^{-12}
Carsi ⁵	SM	9.39×10^{-12}
N95/KN95/FFP		
Study	Mask description	Permeability (m ²)
Ramirez ⁶	3M 8510 (N95)	6.61×10^{-13}
	Moldex 2200 (N95)	2.47×10^{-13}
Du ¹	N95	2.6×10^{-13}
Arden-Dryer ⁷	HDX (N95)	2.71×10^{-12}
	AOXING (KN95)	1.57×10^{-12}
	NANO (KN95)	6.37×10^{-12}
	ARUN (KN95)	1.82×10^{-12}
Duncan ²	N95 3M 8110s	1.18×10^{-11}
	N95 3M 1870	2.76×10^{-12}
	N95 3M 9210	2.84×10^{-12}
Carsi ⁵	FFP2 (1)	1.39×10^{-11}
	FFP2 (2)	1.33×10^{-11}

area of 0.8% of the total face mask surface was used throughout this work, unless stated differently.

Leakage widths, i.e., distances between the face mask and the facial skin, ranged from sub-millimeter up to some 10–15 mm, depending on the type of face mask and facial features.^{40–43} Air flows through leakages are often modeled by Poiseuille flow, assuming a square opening.⁴¹ We applied Darcy’s law instead, implying a non-specified shape but with a specified total surface area, and potential obstructions present within the leaks (e.g., facial hair, face mask fibers).⁴⁴

With the geometry of peripheral leakages established, Darcy’s law also requires the experimentally unknown permeability of the peripheral leakages. Here, we have applied our hypothesis that breathing while wearing a face mask occurs without an additional physical effort to breathe. We found that this is the case with a permeability value $k_{leak} \geq 10^{-6} \text{ m}^2$.

The full model (face mask + peripheral leakage) was then executed for tidal breathing conditions ($V_E = 6.5 \text{ l min}^{-1}$, $k_{fm} = 7 \times 10^{-12} \text{ m}^2$;

TABLE III. The calculated minute ventilation (l min^{-1}) (without face masks) for several values of P_{muscle} (kPa) and the respiratory rate (RR) (breaths min^{-1}). The value of IE is kept constant at 0.6.

P_{muscle} (kPa)	RR (min^{-1})			
	12	18	24	30
0.49	6.5	9.4	11.9	14.1
0.74	9.7	14.1	17.9	21.2
0.98	13.0	18.7	23.9	28.3
1.23	16.2	23.4	29.8	35.3
1.47	19.5	28.1	35.8	42.4

mask thickness = 0.28 mm; mask surface area = 163 cm²; leakage width = 1 mm; leakage area = 0.8% = 1.3 cm²) and resulted in 0.09% of the total volume of air flowing through the face mask. Figure 3(b) shows the pressure difference across the face mask remaining very small due to the presence of peripheral leakages of the face mask. Increasing the leakage area to 2.6% (4.2 cm²) resulted in 0.03% of the volume of air flowing through the face mask.

As an intermediate conclusion, we state that practically all air flows around the face masks. The consequences for the aerosol volume transmission are examined in Secs. III C and III D.

C. Aerosols and face masks

1. Aerosol distribution profiles

An important parameter of the aerosol capture model is the mass of the aerosols and therefore we have established descriptions of the exhaled aerosol size distribution for different vocal activities (breathing, speaking, singing). The aerosol distribution profiles are depicted in Fig. 4, with the corresponding fitted power laws listed in Table IV. The log–log plot shows the importance of distinguishing the number of

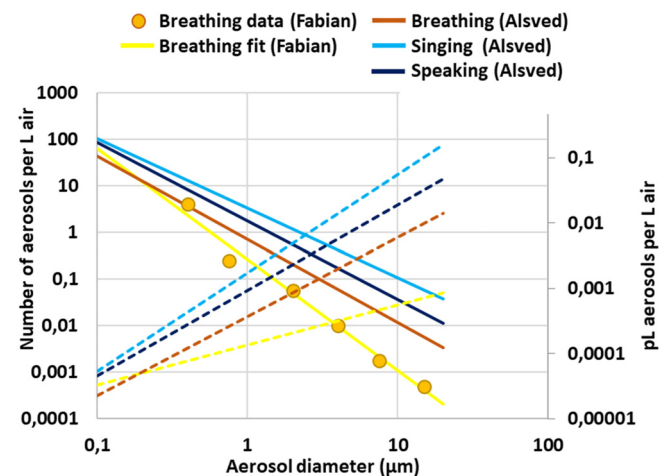


FIG. 4. The aerosol distribution profiles based on the work from Fabian³⁶ and Alved.³⁷ The continuous lines correspond to the left vertical axis (number of aerosols per volume of air) and the dashed lines correspond to the right vertical axis (volume of aerosols in pl per volume of air).

TABLE IV. The power law fits shown in Fig. 4.

Aerosol distribution	Power law fit
Breathing (Fabian <i>et al.</i> ³⁶)	$c_L(d_a) = 0.2593d_a^{-2.381}$
Breathing (Alsved <i>et al.</i> ³⁷)	$c_L(d_a) = \frac{2.9982}{4.23}d_a^{-1.7882}$
Speaking (Alsved <i>et al.</i> ³⁷)	$c_L(d_a) = \frac{7.5445}{4.23}d_a^{-1.689}$
Singing (Alsved <i>et al.</i> ³⁷)	$c_L(d_a) = \frac{13.976}{4.23}d_a^{-1.489}$

aerosols per volume of air from the volume of aerosols per volume of air. Despite the high abundance of small aerosols (diameter 0.1–0.5 μm), their contribution to the overall aerosol volume is very small. On the contrary, the rare large aerosols (diameter >10 μm) still contribute much more to the overall aerosol volume.

2. Minute passing fraction

Next, the aerosol size distribution was combined with the velocity distribution during a breathing cycle. The human breathing profile features different velocity distributions between inhalation and exhalation [Figs. 1(d) and 5]. The aerosol capture efficiency for a specific face mask is primarily a function of the velocity of air and the mass of the aerosol. Figure 5 visualizes the dynamic consequences of these dependencies. An aerosol of 10 μm is completely blocked during inhalation as inhalation is characterized by a high air velocity inward. During the second part of the exhalation phase, the air velocity drops, resulting in a lesser and lesser efficient face mask, down to a point that 10 μm aerosols are no longer effectively blocked. One may notice that when the air flow is low, the displaced volume is small and so the number of 10 μm aerosols may be small as well.

To reduce the parameter space, the temporal variations of the aerosol capture dynamics [Fig. 5(b)] were aggregated by integrating over the number of aerosols passing the face mask (either inward or outward) during one minute of breathing as a function of the aerosol diameter and divide that number by the number of aerosols with the same diameter that would have passed without a mask. This fraction is called the minute passing fraction, analogous to minute ventilation (Fig. 6). Figure 6 indicates whether the minute passing fraction curve shifts toward smaller or larger diameter aerosols as a function of parameters:

1. Density of the aerosols: It means that caution is required when testing a face mask with a low-density aerosol (e.g., soot particles: 0.5 g cm⁻³) and interpreting the result for face mask use against high-density aerosols [e.g., body fluids (1.7 g cm⁻³) or salt crystals (2.1 g cm⁻³)] or vice versa. In general, the calculations indicated that the protective efficiency against air pollution (particulate matter, e.g., aerosols produced by combustion engines) may vary, depending on the chemical composition of the aerosols.
2. Geometrical characteristics of the leakages: Specifically, the percentage of surface area leakage and the width of the gaps (distance between face and the rim of the face mask) are critical. Modeling an increase in the percentage of leaking surface area

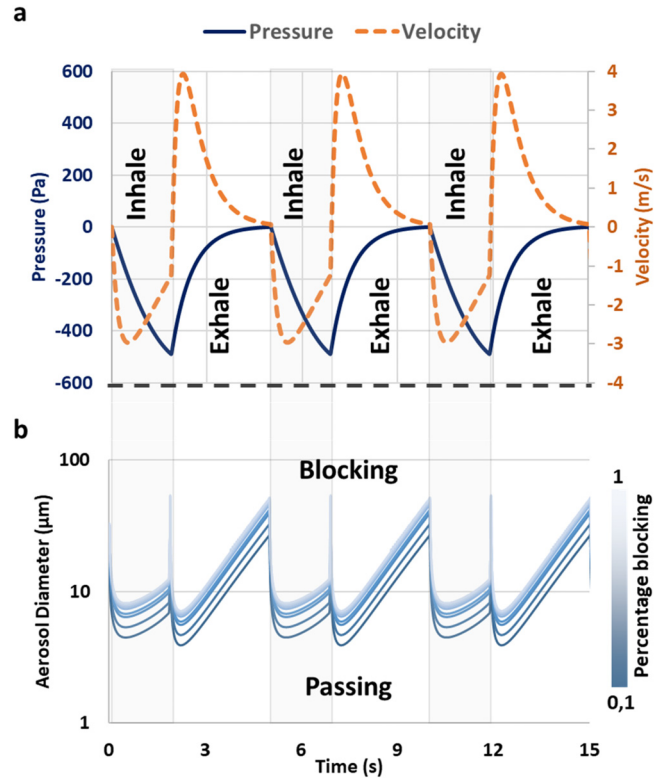


FIG. 5. (a) The relation between the pressure of the diaphragm, the air velocity through the leakages and (b) the aerosol capture efficiency. The contour plot in the lower half shows the gradual transition from 100% aerosol blockage to 10% aerosol passing as a function of the aerosol diameter (vertical axis), in line with the breathing pattern. Tidal breathing conditions: 6.5 l min⁻¹. FFP mask parameters: surface area of the mask = 163 cm², leaking area = 0.8%, leakage width = 1 mm, face mask thickness = 0.28 mm,⁴⁰ permeability of the face mask = 2.7 × 10⁻¹² m², permeability leakage = 10⁻⁶ m².

resulted in a reduction of air flow velocity, while reducing the velocity allowed aerosols with a larger diameter to navigate around the face mask. The same was the case for (implicitly) changing the shape of leakages in the model from slit-like toward

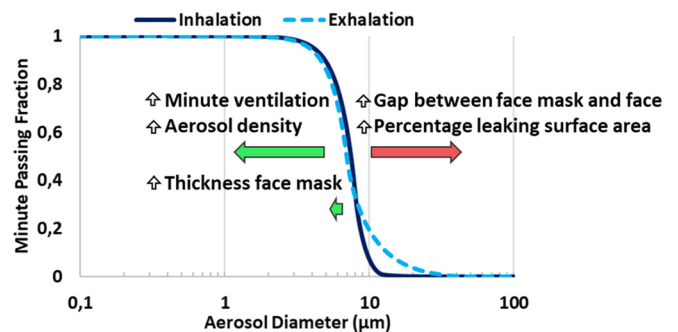


FIG. 6. The minute passing fraction with indications of the direction of the shift of the curve by increasing any of the indicated variables. The small difference between inhalation and exhalation is due to the asymmetric air velocity profile (Figs. 3 and 5).

circular openings (increasing leakage width with constant surface area). The thickness of the edge of the face mask had only a minor influence because the air flow is parallel to the sides of the opening and lateral movement due to diffusion is negligible for $>1 \mu\text{m}$ diameter aerosols.

- Minute ventilation (breathing rate and power): An increase in minute ventilation (i.e., an increase in velocity of air) causes a shift in the cutoff region, toward smaller aerosol diameters, which is effectively the opposite of increasing the percentage of leaking surface area. The result confirmed that increased physical activity improves the effectivity against aerosols passing the face mask during inhalation and exhalation,^{28,29} although facial mimicking and movements of the head may further open up the existing leakages, which could cancel the positive effect of the higher minute ventilation. Although face masks become more effective during increased ventilation rates, the absolute aerosol volume passage is still greater [Fig. 7(a)].

Exhaling features a relatively long period of low velocity air flow when compared to inhalation (Fig. 5). Due to this asymmetric breathing profile, both inhaling and exhaling must be considered separately. The small difference in minute passing fraction curves of inhalation and exhalation contributes to the difference between masking the infectious person and the exposed person (Fig. 6).

The minute passing fraction curve moves to the left when the minute ventilation goes up (Fig. 6), which means that smaller aerosols are effectively blocked. However, an increased minute ventilation also

means a larger volume of air is inhaled/exhaled. The balance between these two effects is shown in Fig. 7(a), showing the difference between the fraction [Fig. 7(a-I)] and absolute volume of aerosols [Fig. 7(a-II)] for a range of leakage widths with different ventilation rates for exhalation. Tidal breathing ($V_E = 6.51 \text{ min}^{-1}$) and a width of 5 mm (0.8% total leaking surface area) resulted in 81% of the aerosol volume passing the face mask, while during heavy work ($V_E = 51 \text{ l min}^{-1}$) and a 10 mm wide leak, only 50% of the exhaled aerosol volume passed the face mask [Fig. 7(a-I)]. Still, the total exhaled aerosol volume was approximately 4.5 times higher for heavy work in combination with a 10 mm leak (2.8 pl min^{-1}) when compared to tidal breathing with a 5 mm leak (0.6 pl min^{-1}) [Fig. 7(a-II)]. That is, because of heavy breathing, a greater volume of air is exchanged and, hence, a greater volume of aerosols is released beyond the face mask. The greater volume of exhaled air overcomes the improved efficiency of the face mask under heavier breathing (due to higher air flow).

Challenging face masks with different aerosol size distributions (0.8% surface area leakage; tidal breathing) produced roughly equal aerosol volume fraction curves [Fig. 7(b-I)], but the difference in aerosol volume was almost a factor 110 between the tidal breathing distribution from Fabian³⁶ (10 mm leakage width, 0.67 pl min^{-1}) and singing (10 mm gap, 78 pl min^{-1}) [Fig. 7(b-II)].

In Sec. III D, we combined the effects of minute ventilation and vocal activity with an environmental effect (evaporation) and computed the total volume of aerosols transmitted between two individuals for several mask-wearing scenarios.

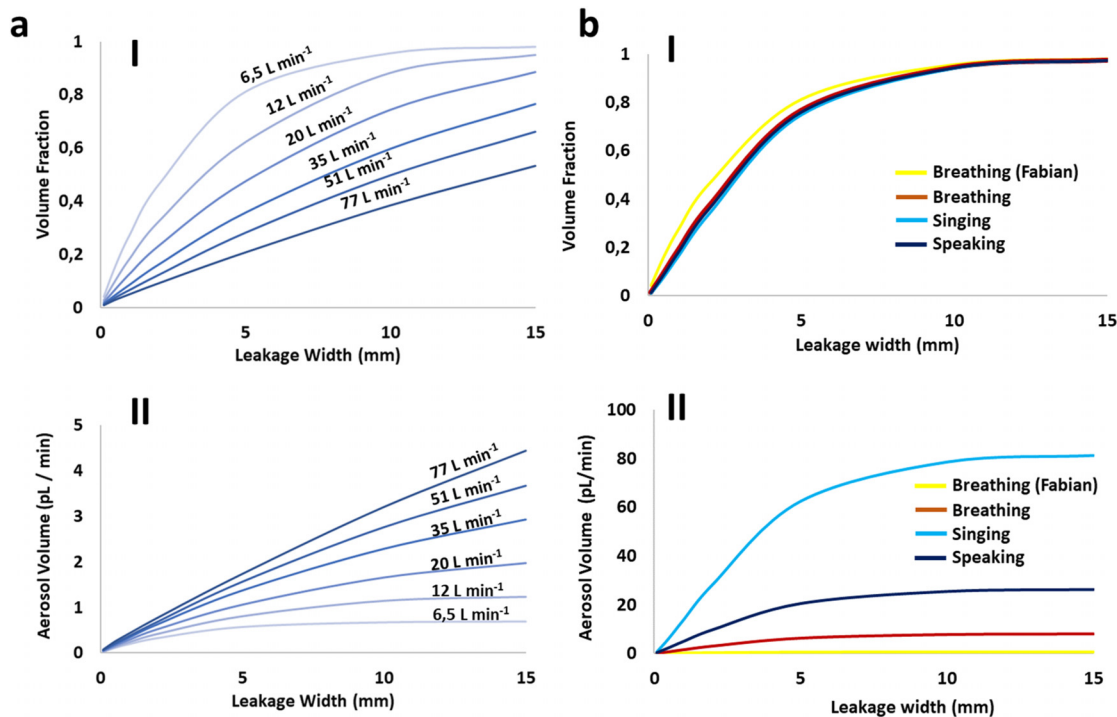


FIG. 7. (a) Challenging a face mask with the aerosol volume distribution (breathing from Fabian *et al.*) with different minute ventilation (V_E) rates (exhalation)³¹ shown as fraction (I) and in absolute volumes per minute (II). (b) Challenging a face mask with different aerosol size distributions ($V_E = 6.5 \text{ l}$) shown as fraction (I) and in absolute volumes per minute (II).

D. Aerosol volume transmission between two persons

The calculation of the effects of wearing vs not wearing a face mask on aerosol volume transmission from one person (infectious, e.g., SARS-CoV-2 positive) to another (exposed) was based on the conceptual aerosol volume transmission model (Fig. 2). Three strongly simplified scenarios (choir, hospital, gym) were selected, in an attempt to single out the influence of face masks for a very specific parameter set. It was assumed that just two people were present in the room, where both the infected and the exposed person were wearing no mask, an SM, or an FFP mask (Fig. 8). The masks were solely defined by their leakage area and width [Fig. 8(a)] because air flow through the mask fabric was negligible. Different activities were chosen because of the difference in minute ventilation and aerosol size distribution [Fig. 8(b)].

The difficulty of assessing the impact of face masks on infection prevention can be explained by recognizing that the effectiveness of

face masks simply depends on numerous parameters, including the activities of all individuals involved (Fig. 8). In fact, the effectiveness of face masks is likely to vary from one person to another in the same room. For example, in the case of an active health care worker (HCW) (light work, breathing) and a patient at rest (tidal breathing) in a hospital, the infectious–exposed scenarios are not equivalent [Figs. 8(d) and 8(e)] because of the difference in physical activities. In other words, asymmetric transmission occurs. In the case of the HCW being infectious, but wearing a FFP mask, the patient without a mask is inhaling 13% (0.09 pl min⁻¹) of the total aerosol volume from the HCW. In case the patient is infectious and the HCW is still wearing an FFP mask, the HCW is inhaling 48% (1.06 pl min⁻¹) of the total aerosol volume from the patient. Similar observations were made for the case of an athlete (heavy work, speaking)–instructor (light work, speaking) in a gym [Figs. 8(f) and 8(g)].

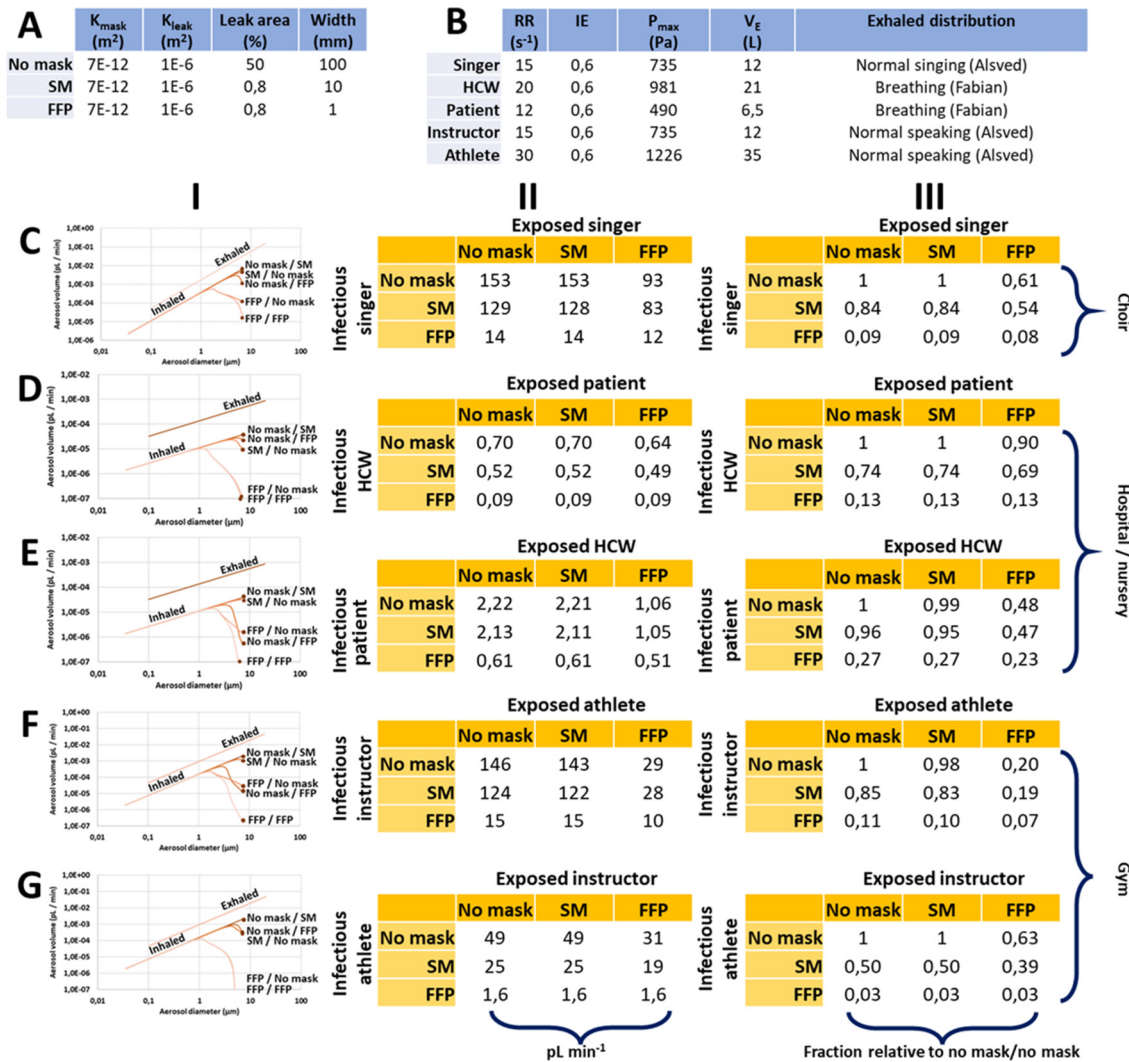


FIG. 8. Aerosol transmission (volume/fraction) results for various scenarios. (a) The properties defining the face masks. (b) The properties defining the different persons. (c)–(g) Various scenarios of the combination of an infectious and exposed person.

In both cases, we stress that we are solely evaluating the impact of face masks on the transmission of aerosols. Proximity effects and ventilation are likely to significantly reduce the absolute aerosol volume inhaled by the exposed persons, but quantifying this effect is beyond the scope of the present work. We did not include irregular breathing patterns during singing or speaking, which is likely to further influence the aerosol volume transmission. Both singing and speaking exhibit a relatively long and constant exhalation phase and a short, powerful inhalation phase in each breathing cycle. Prolonged exhalation with a low air flow promotes the escape of aerosols around the face mask, while powerful inhalation of air improves the efficiency of blocking aerosols.

The type of mask (SM/FFP) is most critical for the infectious person, because fewer or smaller leakages (FFP) increase the air flow velocity and subsequently increase the efficiency of capturing aerosols. Moreover, the aerosol size reduction due to evaporation after passing the source-face mask reduces the capture probability by the face mask of the exposed person.

We point out that expressing the aerosol reduction of face masks in percentages is insufficient to describe the reduction in aerosol volume transmission. When comparing columns II and III [Figs. 8(c)–8(g)], it is clear that, regardless of the reduction factor of 0.08 (choir–FFP/FFP masking), still potentially a larger transmission of aerosol volume (12 pl min^{-1}) is achieved than in the case of a reduction factor of 0.23 (infectious patient and HCW–FFP/FFP masking; 0.51 pl min^{-1}). The physical activities (minute ventilation of both persons and aerosol distribution of the infectious person) are important determinants.

IV. DISCUSSION AND CONCLUSIONS

A. Breathing resistance

The permeability values in the literature (Table III) are surprisingly small and would make breathing through the face mask fabric very hard without leakages. Indeed, rhino manometer measurements of persons wearing SM⁴⁵ or N95 masks⁴⁶ reported an increase in breathing resistance between 120% and 180% and a reduction of inhaled volume of air between 5% and 90%. A reduction of the inhaled volume of air will be compensated for by an increased breathing effort (muscle pressure, breathing rate), which is perceived as hindered breathing.

On the contrary, other studies reported that wearing an FFP mask does not change the physiological, subjective, or behavioral measurements on human subjects in practice.³⁹ It is noted that rhino manometers provide additional sealing of the face mask edges and thus likely enforce breathing through the face mask fabric.

These experimental observations from literature support our modeling result: that the breathing resistance of face masks is very high, but the negative effect on breathing is diminished by the leakages. Practically all air flows through the leakages as air chooses the path of least resistance. This fits with daily life experiences because air escaping around the sides of the face masks explains why it is not possible to blow out a candle when wearing a face mask, why glasses become fogged and why dust is collected around the edges of the face mask when working in a dusty environment for some time.

When establishing that air flows around the face masks, it is implied that the aerosol filtering mechanisms are different from the general ideas. Therefore, critical parameters of the aerosol filter process must be reevaluated as is further discussed in Sec. IV B.

B. Real aerosol volume transmission

The complex interplay between breathing dynamics, the aerosol size distribution, and the geometry of the leakages does not allow a simple intuitive assessment of aerosol volume transmission between two persons (Figs. 2 and 8) for a range of circumstances (i.e., scenarios). We stress that many additional factors should be considered when translating our results to real-world situations such as specific face mask dimensions and leakage geometries and obstructions within the openings (e.g., hair, skin roughness, fibers), breathing through the nose, variable breathing rates when varying physical activities (e.g., sitting, standing, walking, dancing, and sporting), realistically varying breathing patterns related to speaking or singing, occasional coughing or sneezing, temporal variations of the leakage geometries due to physical activities and other influences (e.g., touching the face mask), the relative humidity and temperature over time of the face mask itself and of the space between the wearer and the face mask. All these factors are likely to have an effect on the exhalation and inhalation of aerosol volume but result in an endless list of possible combinations of properties and events. A common theme of these factors is that they are all related to the mask and the wearers.

In addition, the viral load varies by many orders of magnitude³¹ from one person to another, and the viral load depends for each individual on the time after the initial infection. A highly effective face mask may let through only a very small fraction of aerosol volume, which may still carry enough virus particles to cause an infection. In comparison, a face mask that lets through most of the aerosol volume may pose an infection threat when the virus concentration in the aerosols is low. Moreover, room ventilation plays an important role, although room ventilation may potentially keep the average virus concentration in the room low, but in the proximity of the infectious person, the virus concentration is still high.

Therefore, we emphasize that Figs. 8(c) and 8(g) cannot be directly translated to infection risk or serve as a simple explanation for the effectiveness of face masks against infectious diseases. We suspect that the difficulty of finding statistical evidence for the beneficial effects of face masks in cohort studies^{15,16} is related to the intrinsic heterogeneity of the entire transmission process as illustrated in Fig. 2. Based on our work, it is possible to construct much more advanced scenarios, which could include many, if not all, of these additional terms.

C. Renewing face mask concepts

Face masks vary in types of fabric and fitting quality. We have shown that differences in fabrics are irrelevant for aerosol filtration, because the permeability is too small (i.e., breathing resistance is too high). Nevertheless, the diffusive transport properties of fabrics may still play an important role in comfort of wear because of the temperature and water vapor management of the space between the face mask and the face.⁵⁰ Otherwise, the exterior of face masks could be made out of an easy-to-clean, non-deformable layer of plastic and the inside could be covered with something like a reusable, washable insert.

The fitting quality (i.e., leakages) is the only face mask property that plays a role in the efficiency of aerosol retention, which is even more than previously thought.^{25–29} An additional complication arises from the dependency on facial features.^{41–44} Leakages around the face mask are not only inevitable but are also indispensable. Current face mask design aims toward minimization of leakages. Instead, our work suggests that deliberate leakages could be part of the design. Leakages

created in the face mask should allow sufficient air flow without requiring additional physical effort for breathing. Meanwhile, leakages could be designed following the inertial impaction principles,⁵¹ being specifically tuned for the intended aerosols filter properties.

Our new insights regarding the role of leakages bear consequences for the current certification process (NEN-EN 149) and typical investigations, which largely focuses on the fabric of the face mask.^{5–12} We propose that the breathing resistance should be measured without sealing the face mask to the Sheffield head (i.e., dummy) with adhesive tape. The breathing resistance caused by the leaking face mask should remain approximately zero. Moreover, we propose that the fit test (i.e., inward leakage test) is combined with the breathing resistance test, placing the Sheffield head in an enclosed environment with temperature and relative humidity control and a predetermined size distribution of aerosols. Mechanical breathing through the face mask should represent different physical activities. Measurements of the aerosol size distribution behind the face mask can be done with an aerodynamic particle sizer (APS), of which the inlet volume and sample frequency should be in tune with the breathing frequency.⁴⁷ We note that the aerosol size distribution is unstable in time, due to evaporation/condensation processes, depending on the temperature and relative humidity conditions. Moreover, coalescence may occur, in particular with relatively high concentrations of aerosols, which may occur in the leakage openings and the tubing toward the APS. We anticipate that measurements will need to be compared against reference measurements from the same experimental setup.

Face mask quality can be quantified by the aerosol diameter cut-off point (Fig. 6) for a specified breathing pattern, allowing quality labels analogous to pm_{10} , $\text{pm}_{2.5}$, down to “ultrafines” (sub-micron). It must be understood that the label would indicate the smallest aerosol to be blocked, implying that smaller aerosols do pass the face mask. Here, we note that a quantitative microbial risk assessment (QMRA)⁵¹ differs from a particle toxicology risk assessment.⁵² A QMRA requires the cumulative aerosol volume, assuming that the volume scales with the viral load, as input for the dose–response relation. Particle toxicology requires the delivered dose (i.e., numbers of aerosols) as input for the dose–response relation. Therefore, further specifications of the face mask depend on the intended use, i.e., protection against biological threats or protection against particulate matter/ultrafines.

Our work bears implications for washing and reusing practices,^{13,14} as washing is thought to have a negative impact on breathability and particle filtration properties. The latter is caused by the loss of electrostatic charges present in the face mask fabric due to the surfactants present in detergent.¹⁴ With air exclusively passing around the face masks, through the leakages, most of the concerns become obsolete, with the exception of the fitting quality. Reusing face masks would be a major relief for the environmental burden of global face mask use.^{1,2}

In summary, face masks work, but with a different mechanism from what is generally considered. The effectivity against virus transmission is likely to vary significantly from person to person, as both the fitting quality (number of leakages) and the person’s activity (both physical and vocal activity) play a vital role. As a result, asymmetrical transmission occurs, which means that the probability for person A to be infected by person B is not necessarily equal to the probability for person B to be infected by person A under similar circumstances. The asymmetry is further enhanced by differences in immune response due to passed infections and/or vaccinations, or additional risk factors.

We suggest that the asymmetric transmission patterns are likely one of the causes for the epidemiological field studies experiencing difficulties in finding statistically significant differences between wearing and not wearing face masks.

A face mask works most efficiently when the infectious person wears a face mask. Once the aerosol is in the atmosphere, the aerosol evaporates and the resulting smaller aerosol with a relatively high virus concentration is more likely to circumvent the face mask of the exposed person. When both the infectious and exposed person wear a face mask, the aerosol volume transmission is the lowest. Still, over time, an accumulation of aerosol volume will be transmitted. Ultimately, face masks reduce but do not fully prevent exposure.

Based on our findings, we consider that improvements of face mask effectivity against virus transmission is possible by redesigning face masks. It is important to maintain some form of air leakage, but the path can be made more tortuous, as an increased tortuosity increases the effectivity of capturing aerosols.

SUPPLEMENTARY MATERIAL

See the supplementary material for a detailed mathematical description of the thermodynamic constants used throughout the models and a detailed mathematical description of the aerosol capture model.

ACKNOWLEDGMENTS

This study was funded by the Dutch Ministry of Health, Welfare and Sport through the COVID-19 program (Project No. V/190027/22/OM). We thank our internal reviewers Christiaan Delmaar and Hester Volten (RIVM) for their valuable feedback.

AUTHOR DECLARATIONS

Conflict of Interest

The authors have no conflicts to disclose.

Author Contributions

D. A. Matthijs de Winter: Conceptualization (lead); Data curation (equal); Formal analysis (lead); Funding acquisition (equal); Investigation (lead); Methodology (lead); Visualization (equal); Writing – original draft (lead); Writing – review & editing (lead). **Frank M. Verhoeven:** Conceptualization (equal); Investigation (equal); Writing – review & editing (equal). **Lucie C. Vermeulen:** Conceptualization (equal); Funding acquisition (equal); Writing – review & editing (equal). **Erwin Duizer:** Conceptualization (equal); Writing – review & editing (supporting). **Alvin A. Bartels:** Writing – original draft (equal); Writing – review & editing (equal). **Ana Maria de Roda Husman:** Conceptualization (equal); Funding acquisition (lead); Project administration (lead); Supervision (equal); Writing – original draft (equal); Writing – review & editing (equal). **Jack F. Schijven:** Conceptualization (equal); Funding acquisition (equal); Project administration (equal); Supervision (equal); Writing – original draft (equal); Writing – review & editing (equal).

DATA AVAILABILITY

The data that supports the findings of this study are available from the corresponding author upon reasonable request.

REFERENCES

- ¹N. U. Benson, D. E. Bassey, and T. Palanisami, "COVID pollution: Impact of COVID-19 pandemic on global plastic waste footprint," *Heliyon* **7**, e06343 (2021).
- ²B. Li, Y. Huang, D. Guo, Y. Liu, Z. Liu, J.-C. Han, J. Zhao, X. Zhu, Y. Huang, Z. Wang, and B. Xing, "Environmental risks of disposable face masks during the pandemic of COVID-19: Challenges and management," *Sci. Total Environ.* **825**, 153880 (2022).
- ³World Health Organization, see <https://apps.who.int/iris/handle/10665/337199> for "Mask use in the context of COVID-19: Interim guidance" (2020).
- ⁴Y. Cheng, N. Ma, C. Witt, S. Rapp, P. S. Wild, M. O. Andreae, U. Pöschl, and H. Su, "Face masks effectively limit the probability of SARS-CoV-2 transmission," *Science* **372**, 1439–1443 (2021).
- ⁵S. Duncan, P. Bodurtha, and S. Naqvi, "The protective performance of reusable cloth face masks, disposable procedure masks, N95 masks and N95 respirators: Filtration and total inward leakage," *PLoS One* **16**, e0258191 (2021).
- ⁶F. Drewnick, J. Pikkmann, F. Fachinger, L. Moormann, F. Sprang, and S. Borrmann, "Aerosol filtration efficiency of household materials for homemade face masks: Influence of material properties, particle size, particle electrical charge, face velocity, and leaks," *Aerosol Sci. Technol.* **55**, 63–79 (2021).
- ⁷S. Asadi, C. D. Cappa, S. Barreda, A. S. Wexler, N. M. Bouvier, and W. D. Ristenpart, "Efficacy of masks and face coverings in controlling outward aerosol particle emission from expiratory activities," *Sci. Rep.* **10**, 15665 (2020).
- ⁸O. J. Ayodeji, T. A. Hilliard, and S. Ramkumar, "Particle-size-dependent filtration efficiency, breathability, and flow resistance of face coverings and common household fabrics used for face masks during the COVID-19 pandemic," *Int. J. Environ. Res.* **16**, 11 (2022).
- ⁹K. Ardon-Dryer, J. Warzywoda, R. Tekin, J. Biroš, S. Almodovar, B. L. Weeks, L. J. Hope-Weeks, and A. Sacco, Jr., "Mask material filtration efficiency and mask fitting at the crossroads: Implications during pandemic times," *Aerosol Air Qual. Res.* **21**, 200571 (2021).
- ¹⁰W. Du, F. Iacoviello, T. Fernandez, R. Loureiro, J. L. B. Daniel, and P. R. Shearing, "Microstructure analysis and image-based modelling of face masks for COVID-19 virus protection," *Commun. Mater.* **2**, 69 (2021).
- ¹¹M. Carsi and M. Alonso, "Influence of aerosol electrical charging state and time of use on the filtration performance of some commercial face masks for 10–150 nm particles," *J. Aerosol Sci.* **159**, 105849 (2022).
- ¹²V. Varanges, B. Caglar, Y. Lebaupin, Y. T. Batt, W. He, J. Wang, R. M. Rossi, G. Richner, J.-R. Delaloye, and V. Michaud, "On the durability of surgical masks after simulated handling and wear," *Sci. Rep.* **12**, 4938 (2022).
- ¹³A. Peters, R. Palomo, H. Ney, N. Lotfinejad, W. Zingg, P. Parneix, and D. Pittet, "The COVID-19 pandemic and N95 masks: Reusability and decontamination methods," *Antimicrob. Resist. Infect. Control* **10**, 83 (2021).
- ¹⁴H. E. Whyte, A. Joubert, L. Leclerc, G. Sarry, P. Verhoeven, L. Le Coq, and J. Pourchez, "Reusability of face masks: Influence of washing and comparison of performance between medical face masks and community face masks," *Environ. Technol. Innovation* **28**, 102710 (2022).
- ¹⁵R. Chou, T. Dana, and R. Jungbauer, "Update alert 8: Masks for prevention of respiratory virus infections, including SARS-CoV-2, in health care and community settings," *Ann. Intern. Med.* **175**, W108 (2022).
- ¹⁶K. L. Andrejko, J. M. Pry, J. F. Myers, N. Fukui, J. L. DeGuzman, J. Openshaw, J. P. Watt, J. A. Lewnard, and S. Jain, "Effectiveness of face mask or respirator use in indoor public settings for prevention of SARS-CoV-2 infection—California, February–December 2021," *Morb. Mortal. Wkly. Rep.* **71**, 212–216 (2022).
- ¹⁷S. E. Eikenberry, M. Mancuso, E. Iboi, T. Phan, K. Eikenberry, Y. Kuang, E. Kostelich, and A. B. Gumel, "To mask or not to mask: Modeling the potential for face mask use by the general public to curtail the COVID-19 pandemic," *Infect. Dis. Model.* **5**, 293–308 (2020).
- ¹⁸B. Pushpawela, S. Amanatidis, Y. Huang, and R. C. Flagan, "Variability of the penetration of particles through facemasks," *Aerosol Sci. Technol.* **56**, 186–203 (2022).
- ¹⁹L. T. Hirschwald, S. Herrmann, D. Felder, A. M. Kalde, F. Stockmeier, D. Wypyssek, M. Alders, M. Tepper, J. Rubner, P. Brand, T. Kraus, M. Wessling, and J. Linkhorst, "Discrepancy of particle passage in 101 mask batches during the first year of the Covid-19 pandemic in Germany," *Sci. Rep.* **11**, 24490 (2021).
- ²⁰J. T. J. Ju, L. N. Boisvert, and Y. Y. Zuo, "Face masks against COVID-19: Standards, efficacy, testing and decontamination methods," *Adv. Colloid Interface Sci.* **292**, 102435 (2021).
- ²¹R. B. Patel, S. D. Skaria, M. M. Mansour, and G. C. Smaldone, "Respiratory source control using a surgical mask: An in vitro study," *J. Occup. Environ. Hyg.* **13**, 569–576 (2016); Erratum in: *J. Occup. Environ. Hyg.* **19**, 409 (2022).
- ²²H. Ueki, Y. Furusawa, K. Iwatsuki-Horimoto, M. Imai, H. Kabata, H. Nishimura, and Y. Kawaoka, "Effectiveness of face masks in preventing airborne transmission of SARS-CoV-2," *mSphere* **5**, e00637-20 (2020).
- ²³J. T. Brooks, D. H. Beezhold, J. D. Noti, J. P. Coyle, R. C. Derk, F. M. Blachere, and W. G. Lindsley, "Maximizing fit for cloth and medical procedure masks to improve performance and reduce SARS-CoV-2 transmission and exposure," *Morb. Mortal. Wkly. Rep.* **70**, 254–257 (2021).
- ²⁴C. M. de Araujo, O. Guariza-Filho, F. M. Gonçalves, I. B. Basso, A. G. D. Schroder, B. L. Cavalcante-Leão, G. C. Ravazzi, B. S. Zeigelboim, J. Stechman-Neto, and R. S. Santos, "Front lines of the COVID-19 pandemic: What is the effectiveness of using personal protective equipment in health service environments?—A systematic review," *Int. Arch. Occup. Environ. Health* **95**, 7–24 (2022).
- ²⁵S. A. Grinshpun, H. Haruta, R. M. Eninger, T. Reponen, R. T. McKay, and S.-A. Lee, "Performance of an N95 filtering facepiece particulate respirator and a surgical mask during human breathing: Two pathways for particle penetration," *J. Occup. Environ. Hyg.* **6**, 593–603 (2009).
- ²⁶G. Bagheria, B. Thiedea, B. Hejazia, O. Schlenzeka, and E. Bodenschatz, "An upper bound on one-to-one exposure to infectious human respiratory particles," *Proc. Natl. Acad. Sci.* **118**, e2110117118 (2021).
- ²⁷L. H. Kwong, R. Wilson, S. Kumar, Y. S. Crider, Y. R. Sanchez, D. Rempel, and A. Pillarsetti, "Review of the breathability and filtration efficiency of common household materials for face masks," *ACS Nano* **15**, 5904–5924 (2021).
- ²⁸X. Q. Koh, A. Sng, J. Y. Chee, A. Sayovov, P. Luo, and D. Daniel, "Outward and inward protection efficiencies of different mask designs for different respiratory activities," *J. Aerosol Sci.* **160**, 105905 (2022).
- ²⁹N. Chuanxin, T. Solano, K. Shoel, and S. Jung-Hee, "Face masks provide high outward protection despite peripheral leakage: Insights from a reduced-order model of face mask aerodynamics," *Phys. Fluids* **35**, 061911 (2023).
- ³⁰J. Öhman, P. Gren, M. Sjö Dahl, and T. S. Lundström, "Experimental investigation of face mask filtration in the 15–150 μm range for stationary flows," *J. Appl. Phys.* **131**, 044702 (2022).
- ³¹J. F. Schijven, L. C. Vermeulen, A. Swart, A. Meijer, E. Duizer, and A. M. de Roda Husman, "SARS-CoV-2 via breathing, speaking, singing, coughing, and sneezing," *Environ. Health Perspect.* **129**, 047002 (2021).
- ³²A. Albanese, L. Cheng, M. Ursino, and N. W. Chbat, "An integrated mathematical model of the human cardiopulmonary system: Model development," *Am. J. Physiol.: Heart Circ. Physiol.* **310**, 899–921 (2016).
- ³³D. Campbell and J. Brown, "The electrical analogue of lung," *Br. J. Anaesth.* **35**, 684–692 (1963).
- ³⁴A. B. Yildiz, "Modified nodal analysis-based determination of transfer functions for multi-inputs multi-outputs linear circuits," *Automatika* **51**, 353–360 (2010).
- ³⁵B. T. H. Borgelink, A. E. Carchia, J. F. Hernández-Sánchez, D. Caputo, J. G. E. Gardieniers, and A. Susarrey-Arce, "Filtering efficiency model that includes the statistical randomness of non-woven fiber layers in facemasks," *Sep. Purif. Technol.* **282**(Part A), 120049 (2022).
- ³⁶P. Fabian, J. Brain, E. A. Houseman, J. Gern, and D. K. Milton, "Origin of exhaled breath particles from healthy and human rhinovirus-infected subjects," *J. Aerosol Med. Pulm. Drug Delivery* **24**, 137–147 (2011).
- ³⁷M. Alsved, A. Matamis, R. Bohlin, M. Richter, P.-E. Bengtsson, C.-J. Fraenkel, P. Medstrand, and J. Löndahl, "Exhaled respiratory particles during singing and talking," *Aerosol Sci. Technol.* **54**, 1245–1248 (2020).
- ³⁸U.S. Environmental Protection Agency (EPA), *Exposure Factors Handbook*, 2011 ed. (EPA, 2011), Chap. 6.
- ³⁹R. P. Spang and K. Pieper, "The tiny effects of respiratory masks on physiological, subjective, and behavioral measures under mental load in a randomized controlled trial," *Sci. Rep.* **11**, 19601 (2021).
- ⁴⁰P. Hariharan, N. Sharma, S. Guha, R. K. Banerjee, G. D'Souza, and M. R. Myers, "A computational model for predicting changes in infection dynamics due to leakage through N95 respirators," *Sci. Rep.* **11**, 10690 (2021).

- ⁴¹T. Solano, R. Mittal, and K. Shoele, “One size fits all?: A simulation framework for face-mask fit on population-based faces,” *PLoS One* **16**, e0252143 (2021).
- ⁴²T.-K. Wang, T. Solano, and K. Shoele, “Bridge the gap: Correlate face mask leakage and facial features with 3D morphable face models,” *J. Exposure Sci. Environ. Epidemiol.* **32**, 735–743 (2022).
- ⁴³J. Xi, K. Barari, X. A. Si, M. Y. A. Jamalabadi, J. H. Park, and M. Rein, “Inspiratory leakage flow fraction for surgical masks with varying gaps and filter materials,” *Phys. Fluids* **34**, 041908 (2022).
- ⁴⁴S. E. Prince, H. Chen, H. Tong, J. Berntsen, S. Masood, K. L. Zeman, P. W. Clapp, W. D. Bennett, and J. M. Samet, “Assessing the effect of beard hair lengths on face masks used as personal protective equipment during the COVID-19 pandemic,” *J. Exposure Sci. Environ. Epidemiol.* **31**, 953–960 (2021).
- ⁴⁵J. Lässig, R. Falz, C. Pökel, S. Fikenzer, U. Laufs, A. Schulze, N. Hölldobler, P. Rüdlich, and M. Busse, “Effects of surgical face masks on cardiopulmonary parameters during steady state exercise,” *Sci. Rep.* **10**, 22363 (2020).
- ⁴⁶H. P. Lee and D. Y. Wang, “Objective assessment of increase in breathing resistance of N95 respirators on human subjects,” *Ann. Occup. Hyg.* **55**, 917–921 (2011).
- ⁴⁷F. K. A. Gregson, S. Sheikh, J. Archer, H. E. Symons, J. S. Walker, A. E. Haddrell, C. M. Orton, F. W. Hamilton, J. M. Brown, B. R. Bzdek, and J. P. Reid, “Analytical challenges when sampling and characterising exhaled aerosol,” *Aerosol Sci. Technol.* **56**, 160–175 (2022).
- ⁴⁸L. Liu, J. Wei, Y. Li, and A. Ooi, “Evaporation and dispersion of respiratory droplets from coughing,” *Indoor Air* **27**, 179–190 (2017).
- ⁴⁹C. Lieber, S. Melekidis, R. Koch, and H. J. Bauer, “Insights into the evaporation characteristics of saliva droplets and aerosols: Levitation experiments and numerical modeling,” *J. Aerosol. Sci.* **154**, 105760 (2021).
- ⁵⁰J. M. Courtney and A. Bax, “Hydrating the respiratory tract: An alternative explanation why masks lower severity of COVID-19,” *Biophys. J.* **120**, 994–1000 (2021).
- ⁵¹T.-C. Le and C.-J. Tsai, “Inertial impaction technique for the classification of particulate matters and nanoparticles: A review,” *KONA Powder Part. J.* **38**, 42–63 (2021).
- ⁵²O. Schmid and F. R. Cassee, “On the pivotal role of dose for particle toxicology and risk assessment: Exposure is a poor surrogate for delivered dose,” *Part. Fibre Toxicol.* **14**, 52 (2017).